J. Physiol. (1974), **293**, *pp.* 325-345
With 6 text-figures
Printed in Great Britain

INFLUENCE OF DENDRITIC LOCATION AND MEMBRANE PROPERTIES ON THE EFFECTIVENESS OF SYNAPSES ON CAT MOTONEURONES

BY J. N. BARRETT* AND W. E. CRILL

From the Departments of Physiology and Biophysics and Medicine, University of Washington School of Medicine, Seattle, Washington 98195, U.S.A.

(*Received 18 January 1973*)

SUMMARY

1. Measurements of the specific membrane properties and neuronal geometry of cat motoneurones were used to calculate the excitatory post-synaptic potentials (e.p.s.p.s) produced by unit (quantal) conductance changes occurring at various locations on the dendritic tree.

2. Calculations demonstrate that conductance changes of 80–190×10^{-10} mho are required to produce e.p.s.p.s having the same rise time and peak amplitude as the quantal e.p.s.p.s recorded in motoneurones by Kuno & Miyahara (1969*b*). Because quantal conductance changes are so large, synaptic activity can significantly reduce the effective specific resistance of the motoneuronal membrane.

3. A quantal conductance change occurring at a high-impedance distal dendritic site is calculated to produce an e.p.s.p. of 15–20 mV peak amplitude at that site. Significant non-linear summation will occur between the e.p.s.p.s produced by conductance changes occurring simultaneously on the same dendritic branch.

4. Calculations which take into account both non-linear summation and the loss of synaptic charge through dendritic membranes predict that for these motoneurones the time integral of soma-recorded quantal e.p.s.p.s originating on distal dendrites should be at least 20 % as great as the time integral of a quantal e.p.s.p. originating directly on the soma. Quantal conductance changes occurring on 76 % of the dendritic tree should produce soma e.p.s.p. time integrals at least 50 % as great as those produced by somatic synapses.

* Present address: Department of Physiology, University of Iowa, Iowa City, Iowa 52240, U.S.A.

INTRODUCTION

Many of the synapses on cat motoneurones are located on the dendrites at distances greater than 200 μm from the soma (Aitken & Bridger, 1961; Conradi, 1969). The contribution of these distant dendritic synapses to neuronal firing has long been a controversial issue. Earlier studies (Coombs, Eccles & Fatt, 1955; Kernell, 1966) estimated values as low as 500–600 Ω cm^2 for the specific membrane resistance (R_m) of cat motoneurones, and led to the hypothesis that synapses at distal locations on the dendritic tree would influence the somatic voltage much less than more proximal synapses. However, Rall (1959, 1962) calculated considerably higher values for R_m (2000–8000 Ω cm^2), and predicted that tonically active dendritic synapses could produce significant depolarization of the motoneurone soma. Recent experimental work demonstrates that R_m for motoneurone dendrites is actually 1800–3000 Ω cm^2 at the resting potential (Lux, Schubert & Kreutzberg, 1970; Barrett & Crill, 1971, 1974), and that the average electrotonic length of most dendrites is less than two space constants (Nelson & Lux, 1970; Burke & ten Bruggencate, 1971; Barrett & Crill, 1974), supporting Rall's suggestion of a more functional role for distant synapses. This study re-evaluates the relationship between synaptic location and synaptic effectiveness using the measurements of dendritic geometry and specific membrane properties reported in Barrett & Crill (1974).

After a synaptic conductance change on a distant dendrite the postsynaptic potential (p.s.p.) recorded at the soma rises more slowly and reaches a smaller peak amplitude than the p.s.p. produced by a similar conductance change occurring directly on the soma (Rall, 1962; Rall, Burke, Smith, Nelson & Frank, 1967; Jack & Redman, 1971*b*). However, the primary determinant of motoneuronal firing rate is the *net* depolarizing current reaching the soma from many synapses (Granit, Kernell & Lamarre, 1966). Thus, we use the *time integral* (rather than the amplitude or rise time) of the predicted somatic p.s.p. in calculating the relative synaptic effectiveness associated with a particular dendritic location. These calculations, which take into account both the non-linear summation of p.s.p.s and the cable properties of the dendrites, indicate that the distant dendritic synapses can have a significant direct effect on the net somatic depolarization and hence the firing rate of the motoneurone.

METHODS

The calculations described below were performed on a PB-440 computer, using matched electrical and geometrical measurements obtained from cat motoneurones as described in the preceding paper (Barrett & Crill, 1974). All calculations assumed that the dendrites of the reconstructed motoneurones terminated in closed ends at their last visible segments. This sealed-end assumption is supported by electrophysiological data reported by Jack, Miller, Porter & Redman (1971). Unless otherwise noted, a uniform R_m value of 2000 Ω cm^2 and a membrane time constant of 5 msec were assumed.

Synaptic effectiveness, $S(X)$

Synaptic effectiveness, $S(X)$, is defined as the time integral of the voltage change produced at the soma by a unit conductance change Δg occurring at a dendritic location X, divided by the time integral of the somatic voltage change expected if the same Δg had occurred directly upon the soma (X denotes the vector from the soma to the dendritic site). $S(X)$ is calculated as the product of two other normalized factors, the charge injection ratio, $J(X)$, and the charge effectiveness ratio $T(X)$:

$$S(X) = J(X).T(X) \tag{1}$$

$J(X)$ specifies the relative amount of synaptic charge injected into the dendrite at X, and $T(X)$ is the normalized fraction of injected charge that reaches the soma.

Charge injection factor $J(X)$

Synaptic current is equal to the product of Δg and the driving potential (Eccles, 1964; Rall, 1967). Since synaptic current flow changes the post-synaptic membrane voltage in a direction that reduces the driving potential, the amount of charge injected into the post-synaptic cell is not a linear function of Δg. Earlier studies of the non-linear relation between current and conductance at synaptic sites (Martin, 1955; Kuno & Miyahara, 1969*a*) referred to this phenomenon as non-linear summation because one effect of the non-linearity is to make the voltage change produced by simultaneous conductance changes less than the sum of the voltage changes produced when the same conductance changes occur asynchronously. However, the basis of the non-linearity, the reduction in driving potential produced by the flow of synaptic current, occurs even when a single quantum of transmitter is released (Rall, 1964), and is especially marked at distal dendritic synapses, where the input admittance is low.

Non-linear summation is calculated as $(1-J(X))$, where $J(X)$, the charge injection ratio, is defined as the amount of charge $Q(X)$ actually injected at a dendritic site X divided by Q_0, the amount of charge that would have been injected if there had been no change in the synaptic driving potential (Q_0 thus equals the charge injected into a synaptic site voltage-clamped to the original resting potential):

$$J(X) = \frac{Q(X)}{Q_0} = \frac{\int_0^\infty g(X, t)\,\{V_0 - V(X, t)\}\,\mathrm{d}t}{\int_0^\infty g(X, t)\,V_0\,\mathrm{d}t} \tag{2}$$

$V(X, t)$ and $g(X, t)$ represent the time courses of the synaptic voltage and conductance changes, respectively, at dendritic location X. V_0 is the difference between the synaptic reversal potential and the original resting potential. Calculations assumed a V_0 value of 70 mV.

Previous treatments of non-linear summation have employed equations derived for steady-state conductance changes (Martin, 1955, 1966; Kuno & Miyahara, 1969*a*). However, since the steady-state assumption does not hold during actual unitary synaptic events, we calculated $J(X)$ for the transient conductance change produced by one quantum of transmitter and for multiples of this quantal conductance change. We assumed (as did Rall, 1967; Jack *et al.* 1971; Kuno, 1971) that the magnitude and time course of a quantal conductance change are the same for somatic and dendritic synapses; i.e. that $g(t)$ is independent of synaptic location.

For these calculations it is sufficiently accurate to approximate $g(t)$ as a square pulse lasting 0·2–0·5 msec, the range of rise times suggested for quantal potentials of somatic origin (Kuno & Miyahara, 1969*a*; Jack & Redman, 1971*b*). The magnitude of the square-pulse conductance change required to depolarize the soma by 100 μV, the average amplitude of a quantal excitatory post-synaptic potential (e.p.s.p.) of somatic origin (Kuno & Miyahara, 1969*a*, *b*), was calculated for a synapse on the soma ($X = 0$) of a motoneurone of 1 MΩ input resistance by numerical solution of the following equation:

$$V(X, t) = \int_0^t h(X, t-\tau)\, g(t)\{V_0 - V(X, \tau)\}\, d\tau, \tag{3}$$

where $h(X, t)$ is the impulse response at X, evaluated as outlined in the Appendix of Barrett & Crill (1974). Calculated magnitudes ranged from 80×10^{-10} mho for a pulse lasting 0·5 msec to 190×10^{-10} mho for a pulse lasting 0·2 msec. Within this range of rise times, the time integral of the conductance pulse is approximately constant at 40×10^{-10} mho-msec.

The time course of a quantal conductance change was also approximated using the following equation (Rall, 1967; Jack & Redman, 1971*a*; Jack *et al.* 1971):

$$g(t) = \bar{g}\alpha^2 \left(\frac{t}{\tau_m}\right) \exp\left(\frac{-\alpha t}{\tau_m}\right), \tag{4}$$

where τ_m is the time constant of the neurone, and α and $\bar{g}$ are parameters that help determine the shape and magnitude, respectively, of the conductance change (see Fig. 3*A*). Values of α and $\bar{g}$ were adjusted to produce a quantal e.p.s.p. (peak amplitude, 100 μV; rise time, 0·3 msec; see above and Fig. 3*B*) in a motoneurone soma with an input resistance of 1 MΩ and a τ_m of 5 msec (motoneurone 1 in Table 1, Barrett & Crill, 1974). The conductance change so calculated also has a time integral of approximately 40×10^{-10} mho-msec.

The values of $g(t)$ obtained in these two ways were inserted into eqn. (3) to calculate the time course of the synaptic potential change, $V(X, t)$, produced at site X by a local quantal conductance change. These values of $g(t)$ and $V(X, t)$ were then used in eqn. (2) to calculate the charge injection ratio $J(X)$.

Charge effectiveness factor $T(X)$

The relative effectiveness of a dendritic charge injection, $T(X)$, is defined as the time integral of the change in somatic voltage produced by charge injected at the dendritic location X, divided by the time integral of the somatic voltage change occurring when the same amount of charge is injected directly into the soma.

Calculation of $T(X)$ is simplified because the resting neurone behaves as a linear system with respect to the distribution of charge (see below). In such a system, the fraction of locally injected charge that passes through the membrane at any other site is independent of the magnitude and time course of the original charge injection.

This linear property ensures that the *time integral* of current flow across the somatic membrane produced by a synaptic even on a dendrite will be independent of the time course of synaptic charge injection. Thus, for any given dendritic location X, the value of $T(X)$ calculated for the relatively simple case of steady charge injection will also equal $T(X)$ for transient synaptic charge injections.

The numerator of $T(X)$, the steady-state voltage change produced at the soma by a constant current injection at X, was obtained by calculating the voltage change at X and then solving for the voltage change in successively more proximal dendritic segments until the soma was reached. The voltage change at X is the product of the injected current and the input resistance at X. This input resistance was evaluated by iterative application of the steady-state cable equation in the manner used previously to predict the steady-state input resistance at the soma (Barrett & Crill, 1974).

The voltage distribution over dendritic segments between the injection site and the soma was calculated by iterative application of the following equation (Rall, 1959):

$$V_{out} = V_{in}\left(\cosh L + \frac{G_T}{G_{inf}} \sinh L\right). \tag{5}$$

Eqn. (5) gives the steady-state voltage (V_{out}) at the proximal (somatic) end of a cylindrical membrane segment in terms of the following parameters: V_{in}, the steady-state voltage at the distal end of the cylinder; L, the electrical length of the segment, equal to the length of the segment divided by its space constant; G_{inf}, the conductance looking into the end of a semi-infinite cylinder with the same diameter and membrane properties ($G_{inf} = \pi d^{\frac{3}{2}}/2\sqrt{(R_m R_a)}$); and G_T, the steady-state conductance to ground seen looking toward the soma from the proximal end of the segment. G_T was obtained by iterative application of eqn. (14) of Barrett & Crill (1974) for $\omega = 0$; other parameters, the diameter of the cylinder d, the length of the segment x, the specific membrane resistance R_m and the cytoplasmic resistivity R_a, were measured or calculated as described in that paper. The voltage change at X (see above) was inserted as V_{in} into eqn. (5) to solve for the terminal voltage V_{out} at the proximal end of segment X. V_{out} calculated for this distal segment became V_{in} for the next more proximal segment, and this procedure was repeated until the soma was reached. This method of calculating the steady-state somatic voltage change automatically accounts for current lost to dendritic side branches since the conductance of these side branches is added to the terminating conductance of segments ending at branch points.

The denominator of $T(X)$, the voltage change produced by injecting the same steady current directly into the soma, is the product of the injected current and the measured somatic input resistance, R_N.

The assumption of linearity used in calculating $T(X)$ is justified for voltages in the critical 10–15 mV range between the resting potential and threshold by the current–voltage relationships measured by Araki & Terzuolo (1962) and Nelson & Frank (1967). However, calculations reported in Kuno & Miyahara (1969*a*) and in Results (Figs. 1*A*, 3*C*) indicate that quantal conductance changes on high-impedance, distal dendrites produce local e.p.s.p.s exceeding 10 mV. Any active conductance changes brought about by these large dendritic e.p.s.p.s could cause deviation from linear behaviour. Several investigators (Ito & Oshima, 1965; Jack *et al.* 1971) have in fact reported slow, small hyperpolarizations following some e.p.s.p.s, perhaps due to activation of a voltage-dependent potassium conductance. However, Jack *et al.* (1971) present other data consistent with linear behaviour at dendritic synapses, and our preliminary, unpublished voltage-clamp data suggest that the imput im-

pedance of the dendrites changes very little for somatic depolarizations up to 30 mV, so that any voltage-dependent conductance changes in the distal dendrites of normal motoneurones are probably small.

RESULTS

Charge injection at dendritic synapses

The continuous curves in Fig. 1*A* plot the calculated time courses of voltage changes occurring at a dendritic synaptic site about 1·6 space constants from the soma (motoneurone 5, Table 1, Barrett & Crill, 1974) following maintained step conductance changes of various magnitudes. The dotted line in Fig. 1*A* marked $n = 1$ is the locus of peak e.p.s.p. amplitudes compatible with the estimated value of the time integral of a quantal conductance change, 40×10^{-10} mho msec (see Methods). Peak amplitude values corresponding to quantal conductance pulses in the physiological range of 0·2–0·5 msec are enclosed within vertical lines (see Methods; Kuno & Miyahara, 1969*a*; Jack & Redman, 1971*b*). Thus a quantal conductance change at the distal dendritic site illustrated here would be expected to generate an e.p.s.p. of 16–20 mV peak amplitude at that site. In contrast, a quantal conductance change originating on the soma produces an e.p.s.p. of only 100–160 μV at the soma (Kuno & Miyahara, 1969*a*, *b*), because the input impedance of the soma is much lower than the input impedance of distal dendrites.

Calculations of the charge injection ratio J for the distal dendritic site of Fig. 1*A* are plotted in Fig. 1*B*. The continuous curves trace the time course of J following step conductance changes of various magnitudes, and the dotted line marked $n = 1$ indicates the J values compatible with the time integral of a quantal conductance change (40×10^{-10} mho msec). At this particular dendritic site quantal conductance changes lasting 0·2–0·5 msec (vertical lines) have charge injection ratios between 0·81 and 0·86. Thus the change in synaptic driving potential brought about by a quantal conductance change at this distal site reduces the amount of charge injected by $(1-J)$, or 14–19 %.

The line marked $n = 1$ in Fig. 2 connects the J values calculated for a quantal conductance change occurring at various sites along the dendrite of Fig. 1. It is evident that J is lowest for synapses located near the dendritic tips, where the input impedance is high (about 170 MΩ), and that J increases rapidly as sites approach the low-impedance soma (1·45 MΩ). For regions within 0·1 space constant of the soma calculated J values for a single quantum are 0·99 or above.

Dendritic voltage and J values were also calculated using the more accurate approximation of $g(t)$ given by eqn. (4). Values of $g(t)$ (Fig. 3*A*) which produce somatic e.p.s.p.s (Fig. 3*B*) similar to recorded quantal

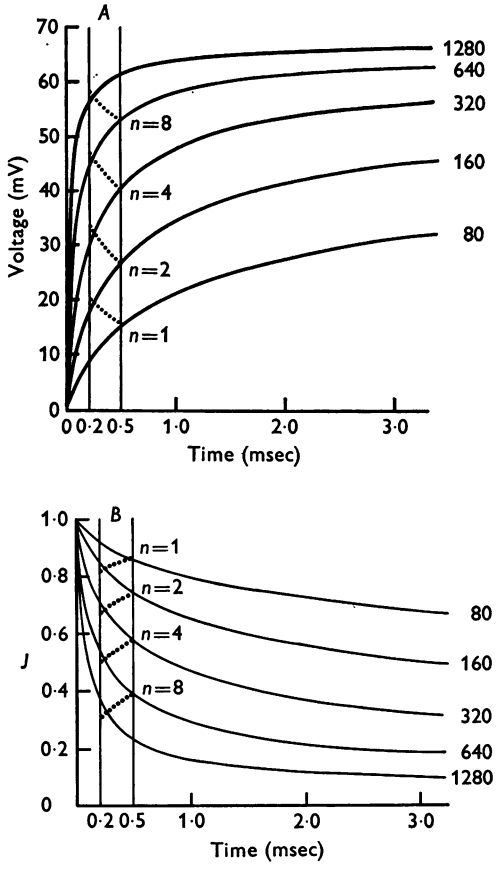

Fig. 1. Calculated time courses (msec) of the voltage change (mV) and charge injection ratio J accompanying localized step conductance changes at a dendritic synapse about 1·6 space constants from the soma of motoneurone 5, Table 1 of Barrett & Crill (1974). The resting input resistance at the dendritic site was 170 MΩ. *A*, continuous curves, calculated using eqn. (3), plot the voltage changes produced by step conductance changes of the indicated magnitudes ($80–1280 \times 10^{-10}$ mho) at this distal dendritic synapse. Vertical lines bracket the physiologically observed durations of a quantal conductance change, 0·2–0·5 msec. Dotted lines indicate the range of peak voltage changes compatible with the simultaneous release of n quanta. *B*, continuous curves, calculated using eqn. (2), plot J for step conductance changes of the indicated magnitudes ($80–1280 \times 10^{-10}$ mho) at this distal synaptic site. Dotted lines indicate the range of J values for a simultaneous conductance changes.

potentials yield values of peak dendritic voltage and J (Figs. 3*C*, *D*) within the range of values calculated assuming square-pulse conductance changes lasting 0·2–0·5 msec (Fig. 1).

Multiple quantal release

Kuno & Miyahara (1969*a*) report that at least 35% of the synapses between Ia afferent fibres and cat motoneurones have average quantal contents (m) of one or less, while about 10% have m values up to 5–15. Because transmission at these synapses is a probabilistic, Poisson process

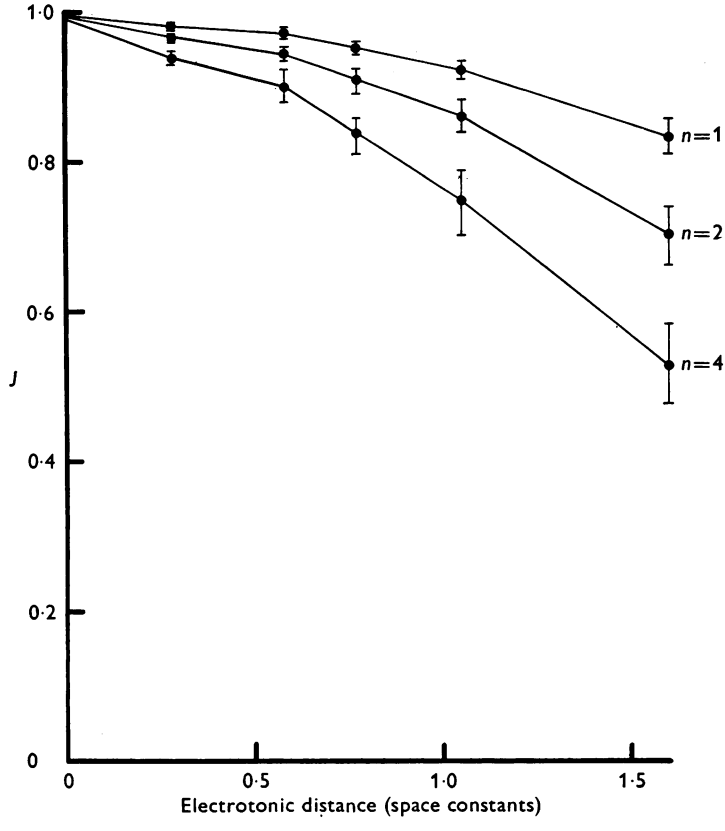

Fig. 2. Charge injection ratio J calculated for dendritic sites at various electrical distances from the soma of motoneurone 5, Table 1, Barrett & Crill (1974). J values were calculated using eqn. (2) for localized (point) quantal conductance changes resulting from the synchronous release of 1, 2 or 4 quanta. For a given quantal number (n), the line connects J values for a 0·3 msec pulse, and brackets delimit J values for conductance pulses lasting 0·2 (lower limit) and 0·5 (upper limit) msec. The dendrite was assumed to terminate in an open circuit at its most distal visible segment, 1·6 space constants from the soma.

(Kuno, 1964), a considerable percentage of afferent action potentials will release multiple quanta, even at terminals where m equals one. Since the amount of charge injected is not a linear function of the synaptic conductance change, J values will depend on the magnitude of $g(t)$. The dotted lines marked $n = 2$, $n = 4$ and $n = 8$ in Fig. 1*B* plot J values for the simultaneous release of 2, 4 or 8 quanta, respectively, at a distal dendritic

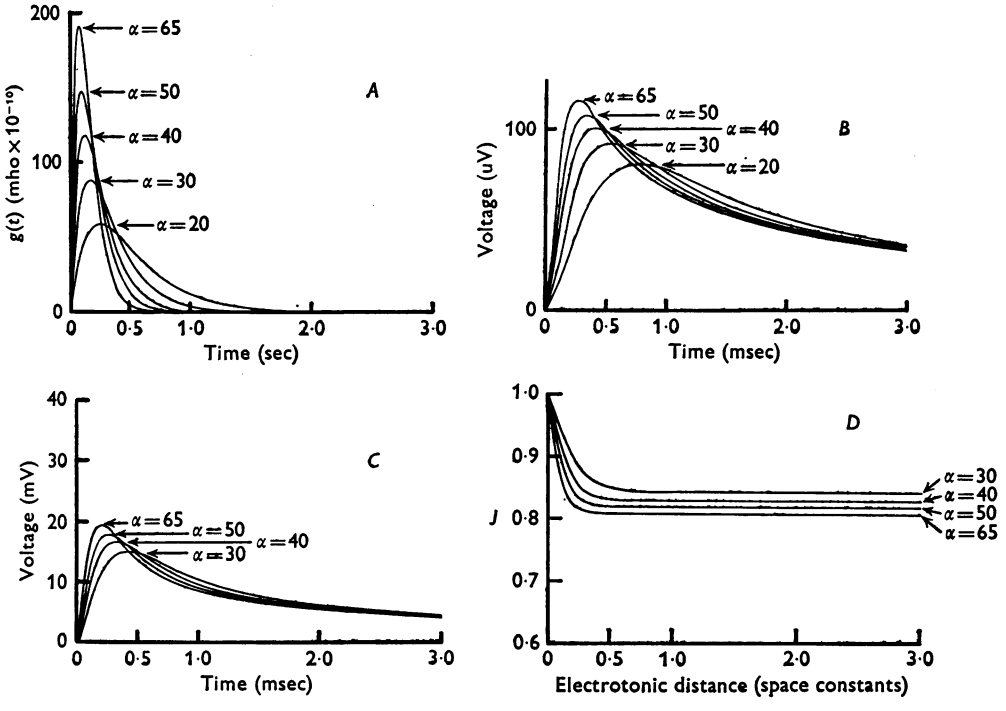

Fig. 3. Predicted synaptic conductance and voltage changes for two sites on motoneurone 5, Table 1, Barrett & Crill (1974). Numbers indicate α values used in calculations. *A*, time course of $g(t)$, the quantal conductance change at a localized post-synaptic site, calculated using eqn. (4). The time integral of $g(t)$ is constant at 40×10^{-10} mho msec for all α (see text), $g(t)$ is assumed to be independent of synaptic location. *B*, time course of the voltage change produced at a synapse on the soma (input resistance 1 MΩ) by the $g(t)$ values plotted in *A*. *C* and *D*, time courses of the changes in voltage and in J, respectively, produced at the distal dendritic site of Fig. 1 (input resistance 170 MΩ) by the $g(t)$ values in *A*, where

$$J(\tau) = \frac{\int_0^\tau g(x, t)\,\{V_0 - V(x, t)\}\,\mathrm{d}t}{\int_0^\tau g(x, t).V_0.\mathrm{d}t}.$$

The J value at the end of the conductance change is the over-all J value used in the text.

site, and lines labelled $n = 2$ and $n = 4$ in Fig. 2 indicate the J values for multiple release at various sites along one particular dendrite. These two Figures show that for a given dendritic location calculated J values decrease as the number of quanta increases, because the increased voltage change produced by the larger synaptic conductance brings about a greater reduction of the synaptic driving potential. Asynchrony in evoked quantal release (Kuno, 1964; Kuno & Miyahara, 1969*a*, *b*) will increase calculated J values.

Charge effectiveness of dendritic synapses

Because the resting motoneurone behaves as a passive, linear, core-conducting system, the charge effectiveness ratio (T) of a given dendritic location is the same, regardless of the magnitude or time course of the dendritic charge injection (see Methods).

Fig. 4 illustrates the calculated steady-state distribution of voltage and charge produced by injecting a steady current of 10^{-10} A into the distal ends of a typical reconstructed dendrite and a semi-infinite equivalent cylinder. About 40% of the current injected into the reconstructed dendrite reaches the soma, a surprisingly large fraction considering that the charge injection site is over 600 μm (about 1·6 space constants) from the soma. In contrast only 20% of the current injected into the sealed end of a semi-infinite equivalent cylinder travels 1·6 space constants before leaking out through the membranes. The efficiency with which the dendrite channels charge into the soma is due mainly to the low input resistance offered by the soma and the other dendrites attached to it. The rapid decrease in input resistance proximal to the charge injection site reduces the integral of the membrane potential change over the membrane area between the injection site and the soma, and hence decreases current loss through intervening dendritic membranes. Dendritic tapering (Barrett & Crill, 1971, 1974) also slightly increases the fraction of dendritic charge reaching the soma. Current lost to side branches (indicated by steps in the current plot of Fig. 4) constitutes only a small fraction (approximately 10%) of the total injected current because the resistance seen looking toward the soma at branch points is low compared to the resistance seen looking toward the tips of the side branches.

Circles in Fig. 5 plot the charge effectiveness ratios (T) calculated for various locations along a multiply-branched dendrite (from neurone 5, Table 1, Barrett & Crill, 1974). T values decrease with the distance from the soma, the lowest values (0·40–0·55 for the dendrite of Fig. 5) occurring at the dendritic tips. The most distal visible segments of dendrites from ten motoneurones had calculated T values ranging from 0·28 for the most distant location (2·2 space constants from the soma) to 0·65 for the closest dendritic termination (0·8 space constants from the soma). These T values

suggest that synaptic charge injected at dendritic terminals will be between 28 and 65% as effective in depolarizing the soma as synaptic charge injected directly into the soma.

Relative effectiveness of dendritic synapses

The triangles in Fig. 5 represent the calculated relative effectiveness (S) of quantal conductance changes occurring along the illustrated multiply branched dendrite. Since both J and T decline with distance from the soma (Fig. 2 and circles of Fig. 5), it follows that their product S also reaches its lowest values (0·20–0·46) at the dendritic tips. S increases rapidly as

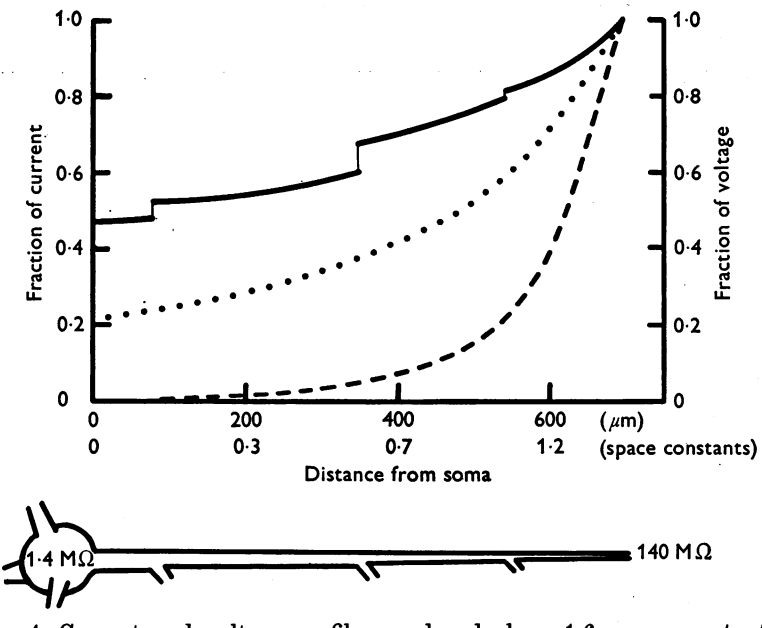

Fig. 4. Current and voltage profiles produced along 1·6 space constant segments of a typical reconstructed dendrite (from motoneurone 5, Table 1, Barrett & Crill, 1974) and a semi-infinite equivalent membrane cylinder by injection of a steady current. Dashed line plots the normalized voltage change (right ordinate) along the reconstructed dendrite; continuous line indicates the fraction of the injected current (left ordinate) remaining in the dendrite at the indicated distance. Steps in the dendritic current record occur at branch points. The schematic drawing of the dendrite below indicates the input resistances at the soma and at the dendritic site of charge injection. Dotted line traces the coincident, normalized current and voltage profiles along the equivalent cylinder. Calculating procedure described in Methods. The large difference between the current profiles along the reconstructed dendrite and the semi-infinite cylinder is due principally to the low-impedance load at the proximal end of the reconstructed dendrite offered by the soma and other dendrites. Effects of dendritic tapering are relatively minor.

synaptic sites approach the soma, and since most of the dendritic area is electrically close to the soma (Fig. 8 of Barrett & Crill, 1974), calculated S values for 76 % of the dendritic area are 0·50 or greater. Earlier calculations by Rall (1962) showed that tonically active synapses on the distal half of an equivalent cylinder (R_m = 2000 Ω cm²) would send 50 % of their current into the soma. The present calculations, based on electrophysiological and geometrical data from the same motoneurones, demonstrate that even an isolated quantal conductance change on the dendrites can have a large relative effect on the net depolarization of the soma.

If some dendritic branches actually continued farther than we could trace them, the distant unseen branches would have S values lower than those calculated here. However, S values for the visible branches would change only slightly, since very little synaptic charge is lost to high-

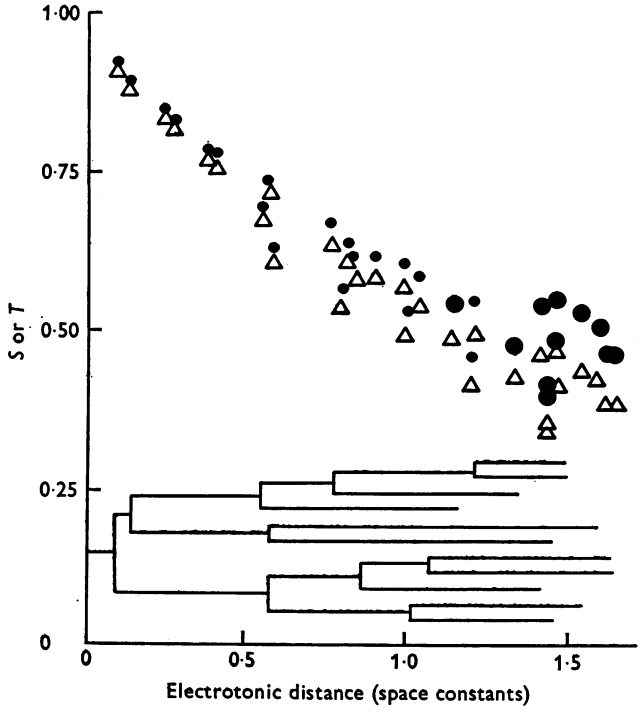

Fig. 5. Circles plot the charge effectiveness ratio T calculated for quantal conductance changes occurring at varying distances along the multiply branched reconstructed dendrite illustrated schematically by the line drawing (from motoneurone 5, Table 1, Barrett & Crill, 1974). Larger circles represent the T values for terminal branches. Triangles plot the relative synaptic effectiveness S at corresponding dendritic sites. Note that sites located at a given electrical distance from the soma have similar, but not identical, T and S values.

impedance dendritic tips. The release of multiple quanta at a given dendritic site reduces the calculated S value because of the high degree of non-linear summation $(1-J)$ at dendritic synapses.

Effect of changes in R_m

The preceding calculations assumed a specific membrane resistance of 2000 Ω cm², but measured resting values of R_m range from 1000 to 3000 Ω cm² (Lux *et al.* 1970; Barrett & Crill, 1971, 1974). A uniform decrease in R_m will occasion a slight increase in the charge injection ratio J, and

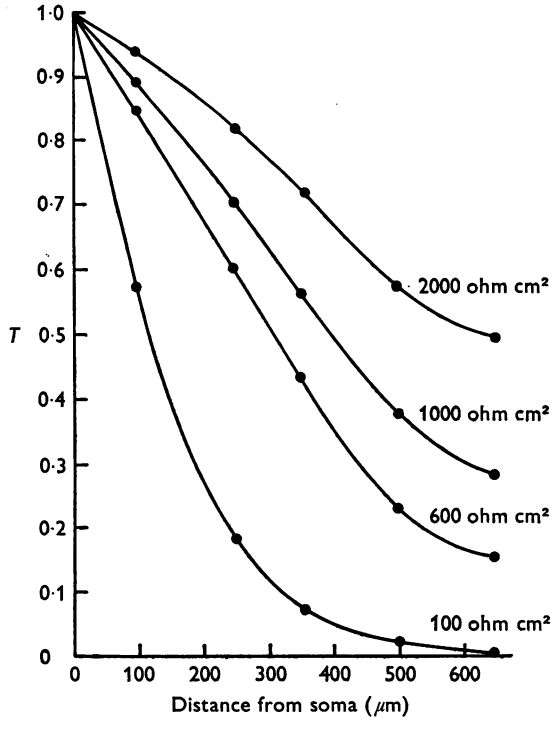

Fig. 6. Effect of R_m on the fraction of injected charge (T) reaching the soma from various sites along a typical dendrite (from motoneurone 1, Table 1, Barrett & Crill, 1974). Lines connect points calculated for the indicated uniform R_m values. Distance from soma in μm.

a greater decrease in the charge effectiveness ratio T, so that the net effect is a decreased synaptic effectiveness S. Fig. 6 shows that reduction in R_m has a greater effect on distal than on proximal synaptic sites. However, T values for even the most distant synapses on the dendrite of Fig. 6 remain quite high ($\geqslant 0{\cdot}3$) for R_m values as low as 1000 Ω cm². Thus

distant synapses should remain effective in depolarizing the soma over the range of R_m values encountered in resting motoneurones.

Synaptic activity can reduce the average effective R_m to values below 1000 Ω cm², and can also change the membrane potential of the neurone. The following hypothetical examples demonstrate that intense synaptic activity reduces the relative effectiveness of neighbouring excitatory synaptic sites.

First, consider the case of excitatory activity localized to a single dendrite. The conductance change brought about by this localized excitatory barrage will reduce the effective R_m (hence altering J and T values) and, in addition, will depolarize the activated dendrite, reducing the driving potential for an e.p.s.p. on that dendrite. This voltage change introduces into the calculation of S an additional factor, the ratio of the synaptic driving potential during the background barrage $(V_0 - \Delta V)$ to the driving potential in the resting dendrite (V_0). Thus, for excitatory synapses on the depolarized dendrite:

$$S(X) = J(X).T(X).(V_0 - \Delta V)/V_0, \tag{6}$$

where ΔV is the steady background level of depolarization at the test site.

The magnitude of the resulting change in S is illustrated by a specific case. Assume that all the synaptic boutons on the dendrite (about 20 boutons per 100 μm² of dendritic membrane, Conradi, 1969) are excitatory, and that each release an average of 15 quanta/sec. This barrage will reduce the effective value of R_m for this particular dendrite to 600 Ω cm² from its original value of 2000 Ω cm². This drop in R_m reduces the product $(J.T)$ for the most distal synapses on the dendrite of Fig. 6 to 0·18 from its original value of 0·34. In addition, the distal portions of the active dendrite are depolarized by about 54 mV, reducing the driving potential for an e.p.s.p. from 70 to 16 mV, for a $((V_0 - \Delta V)/V_0)$ value of 0·23. Thus, from eqn. (6), the new value of S for the tip of the activated dendrite is $(0{\cdot}18 \times 0{\cdot}23) = 0{\cdot}04$; that is, this particular excitatory background barrage will reduce the relative effectiveness of an excitatory quantal conductance change at this distal site from 34 to only 4%.

The second example assumes an intense, mixed excitatory-inhibitory input distributed over the whole neuronal membrane, as might be produced by stimulating the dorsal roots at a high rate (e.g. 1 kHz). We have observed that such a barrage produces little change in V_m, but can drop the measured input resistance to values suggesting average effective R_m values as low as 100 Ω cm². Fig. 6 demonstrates that this low value of R_m drastically reduces T values for all parts of the dendritic tree, especially the more distant synaptic locations.

The preceding analysis focused on excitatory synaptic events, but similar procedures can also be applied to calculate the influence of dendritic location on the relative effectiveness of inhibitory synaptic events. Since the equilibrium potential for i.p.s.p.s is so close to the resting potential, calculations of inhibitory S values must correct for changes in driving potential produced by background activity at neighbouring synaptic sites. For example, the depolarization produced by excitatory activity will significantly increase the effectiveness of simultaneous inhibitory events.

DISCUSSION

Conductance changes underlying quantal p.s.p.s

Calculations presented in Methods demonstrate that a conductance change of $80–190 \times 10^{-10}$ mho is required to produce a 'quantal' e.p.s.p. (peak amplitude 100 μV for motoneurones with $R_N \sim 1$ MΩ, rise time 0·2–0·5 msec, Kuno & Miyahara, 1969*a*, *b*) in our reconstructed motoneurones. This value is much higher than the 17×10^{-10} mho conductance change required to give a steady-state voltage change of 100 μV in similar motoneurones (Kuno & Miyahara, 1969*a*), because much of the current underlying the fast-rising quantal e.p.s.p. goes toward charging the membrane capacitance of the neurone. Kuno & Weakly (1972) estimate that the transient conductance change underlying quantal i.p.s.p.s in motoneurones is even larger than that for quantal e.p.s.p.s. Gage & McBurney (1972) calculate a mean conductance change of 550×10^{-10} mho for the miniature (quantal) end-plate currents in toad skeletal muscle fibres.

The demonstration that a single packet of transmitter produces a conductance change with a time integral of 40×10^{-10} mho msec or more argues that the rate of ongoing synaptic activity has a significant influence on the average effective value of R_m in the motoneurone (see Results).

Non-linear summation and synaptic location

A quantal conductance change is calculated to produce an e.p.s.p. of 16–20 mV in high-impedance distal dendrites (Figs. 1*A*, 3*C*; also Kuno & Miyahara, 1969*a*). This large voltage change significantly reduces the driving potential for the e.p.s.p., and the resulting non-linear relation between synaptic conductance change and synaptic charge injection causes m_{CV} (the value of average quantal content) estimated from the coefficient of variation of e.p.s.p. amplitudes (or areas) to exceed m_F (the value of average quantal content estimated from the proportion of response failures) (Martin, 1955; Kuno & Miyahara, 1969*a*).

We used eqn. (12) in the Appendix to determine which dendritic locations in our reconstructed motoneurones (Barrett & Crill, 1971, 1974) would yield (m_{CV}, m_F) discrepancies similar to those measured by Kuno & Miyahara (1969*a*) for monosynaptic connexions between afferent fibres and motoneurones. Calculations assuming an R_m of 2000 Ω cm^2 placed the most discrepant (m_{CV}, m_F) pairs at high-impedance (input resistance about 70 MΩ) sites located on small dendritic branches 300–500 μm (about one space constant) from the soma. The observation that quantal e.p.s.p.s from these distal, high-impedance sites averaged 60 μV or more at the soma

agrees quite well with the attenuation predicted by the core-conductor model for an R_m of 2000 Ω cm^2, and argues that e.p.s.p.s from such geometrically distant sites can be of significant size at the soma.

Functional importance of non-linear summation

Several factors may reduce the effects of non-linear summation $(1-J)$ on motoneuronal function. First, calculated J values for a single quantal event are at least 0·9 over the proximal 76 % of the dendritic surface area in the motoneurones studied here. Synchronous multiple quantal conductance changes occurring at the same site would reduce J values significantly (Figs. 1*B*, 2), but stimulation of most afferent fibres studied to date releases only one or a few transmitter quanta on a given motoneurone (Kuno & Miyahara, 1969*a*). The degree of non-linear summation between quanta released from neighbouring presynaptic terminals will depend on the synchrony of their activity, as well as on their density, average firing rate and excitatory or inhibitory character.

Dendritic branching reduces the degree of non-linear summation by isolating synaptic conductance changes from each other. Thus, Kuno & Miyahara (1969*a*) observed very little interaction between the synaptic potentials evoked in a motoneurone by stimulating two different afferent fibres, and Burke (1967) observed at most 20 % non-linear summation between synaptic potentials evoked by simultaneous stimulation of two multifibre nerve bundles.

Finally, membrane capacity increases J for synaptic events: J values calculated for brief 'quantal' conductance changes are considerably greater than those for steady-state conductance changes of the same magnitude (Fig. 1*B*). Thus, any geometrical features which increase the effective membrane capacity (e.g. membranous infoldings, dendritic spines, see Gorman & Mirolli, 1972) will increase J (and also S).

Measurement of synaptic effectiveness

The over-all efficacy of a synapse depends on the number of quanta released by the presynaptic terminal, the post-synaptic conductance change produced by each quantum, and the location of the synaptic site (reviewed by Kuno, 1971). Several features combine to make our measure of synaptic effectiveness, $S(X)$, a valid measure of the influence of synaptic location on synaptic function. First, $S(X)$ is defined for the transient conductance change produced by a quantal unit of transmitter, rather than for steady-state conductance changes, because calculations demonstrate the significant effect of the time course of the conductance change on charge injection at dendritic synapses (Fig. 1*B*). Secondly, $S(X)$ is a normalized measure,

comparing dendritic and somatic synapses in terms of their common effect on somatic voltage in order to avoid the complications posed by the different input impedances at these sites.

Finally, $S(X)$ is defined in terms of the *time integral* of the soma-recorded e.p.s.p., rather than its peak amplitude or time course, because the mean current depolarizing the soma (and the nearby axon hillock) is the major determinant of motoneuronal firing rate (Granit *et al.* 1966). The peak amplitude of a unitary e.p.s.p. might be more important than its time integral if unitary e.p.s.p.s were large enough to cross threshold, but these e.p.s.p.s are typically small in motoneurones, and many must sum together to reach threshold (Kuno, 1964; Mendell & Henneman, 1968; Kuno & Miyahara, 1969*a*, *b*). The phenomenon of accommodation indicates that motoneuronal firing rate is sensitive to the rate of change of somatic voltage, but the measured time course of the major components of accommodation (Sasaki & Oka, 1963) is slow compared to the time course of post-synaptic potentials (Rall, 1967, 1970), and the voltage fluctuations of real or artificial synaptic noise increase firing rate only slightly (Granit *et al.* 1966; Calvin & Stevens, 1968; and our unpublished observations).

E.p.s.p.s from distant synapses

Mendell & Henneman (1968) and Mendell & Weiner (1972) used an e.p.s.p. averaging technique capable of detecting e.p.s.p.s too small to be distinguished reliably on a single trial. We used their data to obtain an independent estimate of the relative effectiveness of distant dendritic synapses, as follows:

Assume that Mendell & Henneman's data sample included at least one e.p.s.p. with an average quantal content of one or less that originated on the distal dendrites (at least one space constant from the soma). This assumption seems likely because e.p.s.p.s were measured in 94% of the afferent fibre-motoneurone pairs tested and because quantal contents at such synapses are typically low (Kuno & Miyahara, 1969*a*). The smallest reported averaged e.p.s.p. amplitude was 17 μV; thus, according to our assumption, a quantal release at a distal synapse must produce an e.p.s.p. whose average peak amplitude at the soma is *at least* 17 μV. Kuno & Miyahara (1969*a*, *b*) report an average peak amplitude of 100 μV for quantal e.p.s.p.s of somatic origin, so the ratio of peak amplitudes of distal and proximal quantal e.p.s.p.s is at least 0·17. To convert this amplitude ratio into a ratio of e.p.s.p. areas for comparison with our measure of synaptic effectiveness $S(X)$, we noted that the area-to-peak amplitude ratio for e.p.s.p.s originating more than one space constant from the soma should be at least twice the ratio measured for e.p.s.p.s of somatic origin (measured from Fig. 2 of Rall, 1967). Thus, the ratio of the areas of distal

and proximal e.p.s.p.s is at least 0·34, twice the minimal peak amplitude ratio of 0·17.

Mendell & Weiner compared with the e.p.s.p.s evoked in the soma of a single motoneurone by separate activation of two Ia afferent fibres. We assume that at least one of their e.p.s.p. pairs consisted of an e.p.s.p. of distal origin and an e.p.s.p. of proximal (somatic) origin with similar average quantal contents. Mendell & Weiner's smallest reported peak amplitude ratio was 0·19; according to the above assumption, this is the minimal value of the amplitude ratio of e.p.s.p.s of proximal and distal origin. By reasoning outlined above, this amplitude ratio converts to an e.p.s.p. area ratio of 0·38, another estimate of the synaptic effectiveness of e.p.s.p.s originating at least one space constant from the soma.

In summary, calculations based on the independent observations of Mendell & Henneman and Mendell & Weiner suggest that distal synaptic sites produce a net somatic depolarization at least 34–38 % as great as that produced by somatic sites, percentages in good agreement with the distal $S(X)$ values calculated from motoneuronal geometry and membrane properties (Fig. 5).

APPENDIX

Non-linear summation and estimates of average quantal content

This section derives the equations used to predict the relationship between m_F (the value of average quantal content determined from failures) and m_{CV} (the value of average quantal content calculated from the coefficient of variation of soma-recorded e.p.s.p. amplitudes) for a given dendritic site X.

The expected value of the coefficient of variation (CV) of the amplitudes of e.p.s.p.s originating at a particular synapse is defined as

$$CV = \left[\sum_{n=0}^{\infty} p_n \left(\frac{V_n - \overline{V}}{\overline{V}}\right)^2\right]^{\frac{1}{2}} = \left[\sum_{n=0}^{\infty} p_n \left(1 - \frac{V_n}{\overline{V}}\right)^2\right]^{\frac{1}{2}}, \quad (7)$$

where p_n is the probability that n quanta will be released by a presynaptic action potential, V_n is the peak amplitude of the e.p.s.p. produced by the synchronous release of n quanta, and $\overline{V}$ is the average of the e.p.s.p. amplitudes (V_n and $\overline{V}$ are recorded at the soma).

The charge injected by the release of n quanta at a given site X is proportional to $nJ(X, n)$, where $J(X, n)$ is the charge injection ratio calculated for n quanta at site X using eqn. (2). Because the motoneurone behaves as a linear system at voltages near the resting potential, the peak amplitude of the e.p.s.p. produced at the soma by the release of n quanta at site X will be proportional to the amount of injected charge. Thus:

$$V_n = knJ(X, n), \quad (8)$$

where k is a proportionality constant characteristic of the particular dendritic site and conductance time course. Eqn. (8) applies only to e.p.s.p.s originating at the same synaptic site. The average peak amplitude $\bar{V}$ produced by activation at site X is defined as

$$\bar{V} = \sum_{n=0}^{\infty} p_n V_n = \sum_{n=0}^{\infty} p_n k_n J(X, n). \tag{9}$$

Dividing eqn. (8) by eqn. (9) eliminates the proportionality constant k, yielding:

$$\frac{V_n}{\bar{V}} = \frac{nJ(X, n)}{\sum_{n=0}^{\infty} p_n nJ(X, n)}. \tag{10}$$

Since transmitter release at synapses between Group Ia afferent fibres and motoneurones can be described by Poisson statistics (Kuno, 1964):

$$p_n = \frac{e^{-m} m^n}{n!} \tag{11}$$

where m is the average number of quanta released by nerve stimulation. One estimate of m is m_F, determined from the proportion of trials p_0 on which no quantum is released:

$$m_F = \ln (p_0).$$

Since for a Poisson process m_{CV} is defined as $(CV)^{-2}$, combination of eqns. (7), (10) and (11) allows calculation of the expected relationship between m_F and m_{CV} for a given dendritic site X:

$$\frac{1}{m_{CV}} = (CV)^2 = \sum_{n=0}^{\infty} \left\{ \left(\frac{e^{-m_F} m_F^n}{n!} \right) \left(1 - \frac{nJ(X, n)}{\sum_{n=0}^{\infty} \left(\frac{e^{-m_F} m_F^n}{n!} \right) (nJ(X, n))} \right)^2 \right\}, \tag{12}$$

This series converges rapidly.

We thank Drs W. L. Hardy, B. Hille, C. F. Stevens and J. W. Woodbury for helpful discussion and criticism, Dr T. Kehl and his staff for computer facilities and assistance, Dr M. Heath for help in calculating the complex input admittance of the neurone and Dr E. Barrett for careful reading and editing of the manuscript. Supported by USPHS grants GM 00739, NS 09787, and FR 00374.

REFERENCES

AITKEN, J. T. & BRIDGER, J. E. (1961). Neuron size and neuron population density in the lumbosacral region of the cat's spinal cord. *J. Anat.* **95**, 38–53.

ARAKI, T. & TERZUOLO, C. A. (1962). Membrane currents in spinal motoneurons associated with the action potential and synaptic activity. *J. Neurophysiol.* **25**, 772–789.

BARRETT, J. N. & CRILL, W. E. (1971). Specific membrane resistivity of dye-injected cat motoneurons. *Brain Res.* **28**, 556–561.

BARRETT, J. N. & CRILL, W. E. (1974). Specific membrane properties of cat motoneurones. *J. Physiol.* **239**, 301–324.

BURKE, R. E. (1967). Composite nature of the monosynaptic excitatory postsynaptic potential. *J. Neurophysiol.* **30**, 1114–1137.

BURKE, R. E. & TEN BRUGGENCATE, G. (1971). Electrotonic characteristics of alpha motoneurones of varying size. *J. Physiol.* **212**, 1–20.

CALVIN, W. H. & STEVENS, C. F. (1968). Synaptic noise and other sources of randomness in motoneuron interspike intervals. *J. Neurophysiol.* **31**, 574–587.

CONRADI, S. (1969). On motoneuron synaptology in adult cats. *Acta physiol. scand.* suppl. 332.

COOMBS, J. S., ECCLES, J. C. & FATT, P. (1955). The electrical properties of the motoneurone membrane. *J. Physiol.* **130**, 291–325.

ECCLES, J. C. (1964). *The Physiology of Synapses.* Berlin: Springer-Verlag.

GAGE, P. W. & MCBURNEY, R. N. (1972). Miniature end-plate currents and potentials generated by quanta of acetylcholine in glycerol-treated toad sartorius fibres. *J. Physiol.* **226**, 79–94.

GORMAN, A. L. F. & MIROLLI, M. (1972). The geometrical factors determining the electrotonic properties of a molluscan neurone. *J. Physiol.* **227**, 35–49.

GRANIT, R., KERNELL, D. & LAMARRE, Y. (1966). Algebraical summation in synaptic activation of motoneurones firing within the 'primary range' to injected currents. *J. Physiol.* **187**, 379–399.

ITO, M. & OSHIMA, T. (1965). Electrical behaviour of the motoneurone membrane during intracellularly applied current steps. *J. Physiol.* **180**, 607–635.

JACK, J. J. B., MILLER, S., PORTER, R. & REDMAN, S. J. (1971). The time course of minimal excitatory post-synaptic potentials evoked in spinal motoneurones by Group Ia afferent fibres. *J. Physiol.* **215**, 353–380.

JACK, J. J. B. & REDMAN, S. J. (1971*a*). The propagation of transient potentials in some linear cable structures. *J. Physiol.* **215**, 283–320.

JACK, J. J. B. & REDMAN, S. J. (1971*b*). An electrical description of the motoneurone, and its application to the analysis of synaptic potentials. *J. Physiol.* **215**, 321–352.

KERNELL, D. (1966). Input resistance, electrical excitability, and size of ventral horn cells in cat spinal cord. *Science, N.Y.* **152**, 1637–1640.

KUNO, M. (1964). Quantal components of excitatory synaptic potentials in spinal motoneurones. *J. Physiol.* **175**, 81–99.

KUNO, M. (1971). Quantum aspects of central and ganglionic synaptic transmission in vertebrates. *Physiol. Rev.* **51**, 647–678.

KUNO, M. & MIYAHARA, J. T. (1969*a*). Non-linear summation of unit synaptic potentials in spinal motoneurones of the cat. *J. Physiol.* **201**, 465–477.

KUNO, M. & MIYAHARA, J. T. (1969*b*). Analysis of synaptic efficacy in spinal motoneurones from 'quantum' aspects. *J. Physiol.* **201**, 479–493.

KUNO, M. & WEAKLY, J. N. (1972). Quantal components of the inhibitory synaptic potential in spinal motoneurones of the cat. *J. Physiol.* **224**, 287–303.

LUX, H. D., SCHUBERT, P. & KREUTZBERG, G. W. (1970). Direct matching of morphological and electrophysiological data in cat spinal motoneurons. In *Excitatory Synaptic Mechanisms.* Proc. of the Fifth International Meeting of Neurobiologists, ed. ANDERSEN, P. & JANSEN, J. K. S. Oslo: Universitetsforlaget.

MARTIN, A. R. (1955). A further study of the statistical composition of the end-plate potential. *J. Physiol.* **130**, 114–122.

MARTIN, A. R. (1966). Quantal nature of synaptic transmission. *Physiol. Rev.* **46**, 51–66.

MENDELL, L. M. & HENNEMAN, E. (1968). Terminals of single Ia fibers: Distribution within a pool of 300 homonymous motor neurons. *Science, N.Y.* **160**, 96–98.

MENDELL, L. & WEINER, R. (1972). Convergence of pairs of Group Ia fibers to spinal motoneurons in the cat. *Society for Neuroscience Abstracts*, **209**.

NELSON, P. G. & FRANK, K. (1967). Anomalous rectification in cat spinal motoneurons and effect of polarizing currents on excitatory postsynaptic potential. *J. Neurophysiol.* **30**, 1097–1113.

NELSON, P. G. & LUX, H. D. (1970). Some electrical measurements of motoneuron parameters. *Biophys. J.* **10**, 55–73.

RALL, W. (1959). Branching dendritic trees and motoneuron membrane resistivity. *Expl Neurol.* **1**, 491–527.

RALL, W. (1962). Theory of physiological properties of dendrites. *Ann. N.Y. Acad. Sci.* **96**, 1071–1092.

RALL, W. (1964). Theoretical significance of dendritic trees for neuronal input–output relations. In *Neural Theory and Modeling*, ed. REISS, R. F. Stanford: Stanford University Press.

RALL, W. (1967). Distinguishing theoretical synaptic potentials computed for different soma-dendritic distributions of synaptic input. *J. Neurophysiol.* **30**, 1138–1168.

RALL, W. (1970). Cable properties of dendrites and effect of synaptic location. In *Excitatory Synaptic Mechanisms*, Proc. of the Fifth International Meeting of Neurobiologists, ed. ANDERSEN, P. & JANSEN, J. K. S. Oslo: Universitetsforlaget.

RALL, W., BURKE, R. E., SMITH, T. G., NELSON, P. G. & FRANK, K. (1967). Dendritic location of synapses and possible mechanisms for the monosynaptic EPSP in motoneurons. *J. Neurophysiol.* **30**, 1169–1193.

RALL, W. & RINZEL, J. (1973). Branch input resistance and steady attenuation for input to one branch of a dendritic neuron model. *Biophys. J.* **13**, 648–688.

SASAKI, K. & OKA, H. (1963). Accommodation, local response and membrane potential in spinal motoneurons of the cat. *Jap. J. Physiol.* **13**, 508–522.